*2nd URSI AT-RASC, Gran Canaria, 28 May – 1 June 2018*

# Design of Narrow Band Single-Layer Chipless RFID Tag

Ricardo Figueiredo*[(1,2)], João Louro [(1)], Samuel Pereira [(1,2)], João Gonçalves [(1)], and Nuno Borges Carvalho [(1,2)]
(1) Universidade de Aveiro, Campus Universitário de Santigo, 3810-193 Aveiro, Portugal.
(2) Instituto de Telecomunicações, 3810-193 Aveiro, Portugal.

## Abstract

This paper presents the design of a narrow band single-layer chipless RFID tag based on the coplanar stripline c-section resonator with 3-bit coding capacity.

## 1. Introduction

RFID technology takes advantage of the radar principle for communication purposes. The radar principle can be stated in the following way: an electromagnetic (EM) wave incident on a conducting object will be reflected in accordance with the reflection coefficient that the conducting object presents to the travelling EM wave.

In chipless RFID technology there are no active devices, only passive components are used. A resonator structure is designed so that a specific static electromagnetic signature (EMS) is coded in the reflected signal, this EMS uniquely identifies the chipless RFID tag.

There are several techniques to encode an EMS, the most used are time, phase and frequency encoding techniques. In time encoding techniques, a structure is designed including one, or several delay lines that introduce specific temporal delays on the received signal and then retransmits it, these delays identify the tag. In phase encoding techniques, the resonator structure is designed to introduce phase shifts on the incident EM wave at specific frequencies, these phase shifts identify the tag. In frequency encoding techniques, the resonator structure acts as band-stop filters, resonating at some frequencies and attenuating others, this creates a specific EM spectrum characteristic, the transfer function, that uniquely identifies the tag.

Depending on the type of encoding, a reader can be implemented to detect time delays, phase shifts or spectrum characteristics introduced by the chipless tag. The detection is greatly simplified by the fact that the signals are static, and averaging mechanisms and other techniques [3] can be used to detect the very low power signals transmitted by chipless tags. Tag identification is based on correlation with previously measured tag characteristics. Depending on the tag, environment characterization measurements might or might not be needed [3,4]. Traditionally the metric used to characterize the performance of a tag is radar cross section (RCS) [5,8].

When compared with traditional chipped passive RFID, chipless RFID technology is a lower complexity solution that doesn't require active devices nor power harvester to operate, this makes it a greener solution [8] because it requires less power and less components to operate. The need for less components allied with the possibility of mass production using flexography also drastically reduces the cost of chipless RFID, which is considered extremely low-cost RFID [8]. This allied with sensing capabilities [7] reveals the high potential of this technology, making chipless RFID extremely desirable for IoT solutions.

A more extensive overview of chipless RFID technology is presented in [8]. The following sections of this paper present the designing steps of a frequency encoded narrow band 3-bit single-layer chipless RFID tag, based on coplanar stripline c-section resonator. This design contrasts with traditional chipless tag design, that typically is broadband, and usually struggles to be FCC compliant [4].

## 2. Design

### 2.1 Theory

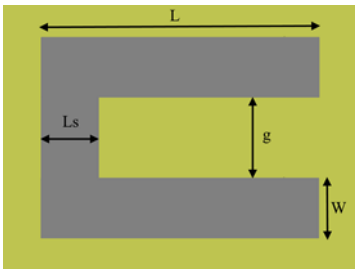


**Figure 1.** C-section resonator.

The basis for the tag design is a c-section resonator. This structure consists on a coplanar stripline terminated in open circuit in one end and terminated in short circuit at the other end [4], as is depicted in figure 1. The c-section resonates at a single frequency band.

Because the aim was to design a tag to operate near the 900MHz band, where backscatter communications are regulated, adjustments in the c-section were made by simulation to design a tag for the desired frequency band. Changing the length of the slot, L, coarsely adjusts the resonance frequency, while changing the length of the short circuit, Ls, finely adjusts the resonance frequency. The gap, g, between lines, and the width of the lines, w, changes the bandwidth of the resonance peaks [9].

To produce multiple resonance peaks, multiple c-section resonators were used as is presented in [9]. But instead of using multiple c-section to obtain abrupt phase changes, the multiple c-section are used to produce multiple resonance peaks with lower bandwidth, due to the abrupt phase changes caused by the multiple c-section resonators. This aid the narrow band tag design.

In the presented design, the dielectric used was single layer FR-4, with 4.4 relative permittivity, 1.6 mm height and 35µm of copper thickness. The use of this low-cost dielectric makes the cost of the tags insignificant.

## 2.2 Simulation

A c-section structure was designed on CST STUDIO SUITE 2017 based on equation (1) for the resonant frequency of 2.45GHz. The initial values of g and w were 0.5mm and 3 mm respectively, as used in [4].
The length of the slot was then optimized to center the resonant frequency around 950MHz. Afterward, g and w values were optimized to maximize quality factor. The values of L, g and w that center the resonator around 950MHz with narrower bandwidth are presented in table 1.

**Table 1.** Optimum values narrow band resonance frequency centered at 950MHz

| | |
|---|---|
| w [mm] | 3 |
| g [mm] | 4.5 |
| L [mm] | 121 |

The next step was to incorporate multiple c-sections on a single tag to obtain multiple resonance peaks. The distance between resonators was optimized to reduce coupling effects. The aim was on trying to incorporate the maximum number of resonance peaks in a bandwidth of 50MHz. Upon the first simulation results it was considered reasonable to implement a system with 3-bits, i.e. three resonances, in a bandwidth of 60MHz. The chosen resonance frequencies were 930MHz, 950MHz and 980MHz.

Table 2 shows short circuit lengths, Ls, to center the resonance peaks at these frequencies, figure 2 shows the layout PCB of the 3-bit tags, and figures 3 shows the RCS simulation results.

**Table 2.** Short circuit lengths for resonant frequencies at 920MHz, 950MHz, and 980MHz

| | |
|---|---|
| Ls_920 [mm] | 66.5 |
| Ls_950 [mm] | 68.3 |
| Ls_980 [mm] | 69.6 |

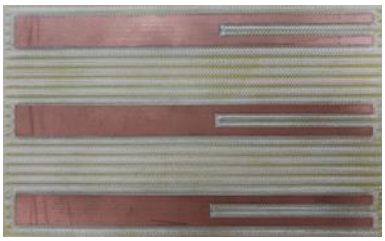

**Figure 2.** 3-bit tag PCB. 920MHz, 950, and 980MHz resonating frequencies.

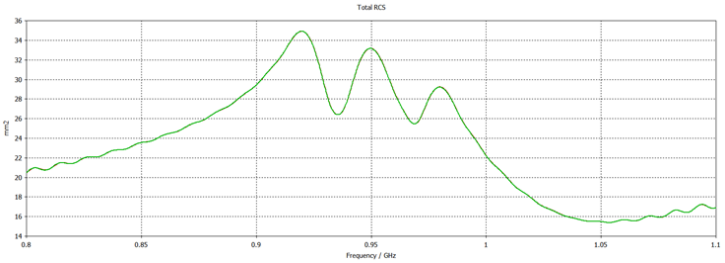


**Figure 3.** 3-bit tag RCS simulation.

The simulation results lead to conclude that it is possible to implement a chipless RFID system capable of coding 3 bits with 60MHz bandwidth centered around 950MHz. The simulation results indicate that tag characterizations will be measurable, because between peaks there are at least 3dB valleys.

## 2.3 Measurements


**Figure 4.** Monostatic RCS measurement setup.

To characterize the designed tags a monostatic RCS measurement setup was used, as depicted in figure 4. The VNA used was Keysight's PNA-X network analyser and the antenna used was a patch antenna centered around 880MHz. The transmitted power by the VNA was 13.4 dBm, this high value is justified by the mismatch of the used antenna for the tags operating frequency.

To extract the RCS from the S11 measurements equation (1) is used, which is based in equation (5) from [4]. The isolation measurement represents a measurement of the environment, the reference measurement represents a measurement of an object with known RCS, a metal plate

was used as described in [4]. This means that for characterizing these tags both environmental and reference measurements are needed for calibration.

$$RCS_{tag} = \left[\frac{S_{11}^{tag} - S_{11}^{isolation}}{S_{11}^{reference} - S_{11}^{isolation}}\right]^2 RCS_{reference} \quad (1).$$

The measurements were performed in laboratorial environment with the help of an absorbing background plane to avoid multipath and the establishment of a standing wave, as depicted in figure 5.

**Figure 5.** Experimental setup.

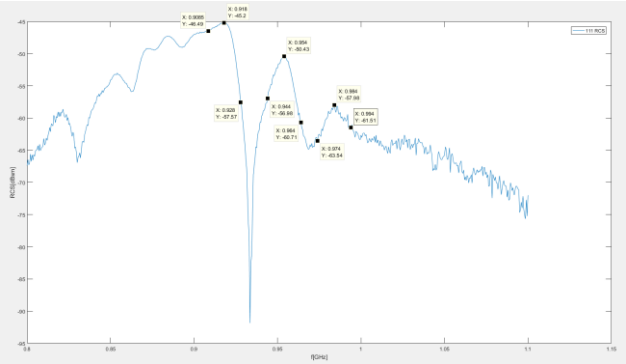

**Figure 6.** 3-bit tag RCS measurement.

## 2.4 Performance Analysis

As can be seen in figures 6, it was possible to characterize the designed tag. The correlation between measurements and simulation is high. The frequency shift when compared with simulation results is 5MHz in a 950MHz carrier, which corresponds to a shift of less than 1%. This confirms that it is possible to design a 3 bit chipless RFID tag with bandwidth 60MHz centered at 950MHz, and that the followed design method can be trusted to produce the expected results.

The used antenna was mismatched for the tag's operating frequencies; however, it was the only directional antenna available in the lab operating around the selected frequency band. This caused some problems in the tag characterization, especially because more power needed to be transmitted by PNA-X to be able to characterize the tag. This slightly fades the evidence of the lower frequency resonance, but the strong pattern of peak-valley, as described in [9], gives confidence that at 920MHz a resonance peak can be found.

Observe that in between peaks and valleys, the measurement results always present at least 3dB margin.

Some state of the art tags are evaluated in terms of spatial and spectral efficiency in figure 22 of [4]. In that figure, the most spatially efficient tag is capable of coding $3\ bits/cm^2$, while the most spectrally efficient tag is capable of coding 25 bits/GHz. The tags presented in this paper is capable of coding $0.028\ bits/cm^2$ and 50 bits/GHz. This means that while the presented design is much larger than the state of the art design it can use spectrum more efficiently. This might be helpful, especially in implementing lower complexity reading systems, which are the most complex part of implementing a chipless RFID system. Other advantage might relate with the ease to obtain FCC compliance to approve future chipless RFID applications.

## 3. Future Work

In the future, it is important to characterize the tags using a better measuring antenna, and repeat the process in anechoic chamber environment. The characterization in anechoic chamber will allow for a better characterization, that then can be used to detect the tags in real world environments without the need for environmental and reference measurements [3].

Another topic of investigation is on different type of resonators. The focus of this investigation is on how other resonating structures can help in the miniaturization of the designed tags. The aim is to achieve spatial efficiency comparable with those presented in state of the art tags, such as those in figure 22 of [4], while maintaining the spectral efficiency of the presented design.

Other path of future investigations will focus on how can the use of narrow band chipless RFID tags simplify the reader architecture of chipless RFID systems.

## 4. Conclusions

In the presented work, a narrow band 3-bit single-layer tag based on c-section resonators was proposed, simulated and measured. The measurements validate the design.

The presented design is suitable to mass production using flexography because it is a single layer design.

This design also has impressive spectral efficiency when compared to state of the art designs, however size reduction is extremely desirable, since the design has poor spatial efficiency.

## 5. Acknowledgements

This work is funded by FCT/MEC through national funds and when applicable co-funded by FEDER – PT2020 partnership agreement under the project UID/EEA/50008/2013

## 6. References

1. M. Friedli, L. Kaufmann, F. Paganini, R. Kyburz, “Energy Efficiency of the Internet of Things: Technology and Energy Assessment Report”, IEA 4E EDNA, April 2016.

2. Silicon Labs, “Battery Size Matters, Five fundamental considerations for battery-powered, wireless IoT sensor product.”.

3. A. Vena, E. Perret, B. Sorli, S. Tedjini, “Toward reliable readers for chipless RFID systems”, 2014 XXXIth URSI General Assembly and Symposium (URSI GASS), August 2014, doi:10.1109/URSIGASS.2014.6929209.

4. A. Vena, E. Perret, S. Tedjini, “Design of Compact and Auto-Compensated Single-Layer Chipless RFID Tag”, IEEE Transactions on Microwave Theory and Techniques, 60, 9, July 2012, pp. 2913-2924, doi:10.1109/TMTT.2012.2203927.

5. D. Kuester, Z. Popovic, “How Good Is Your Tag?: RFID Backscatter Metrics and Measurements”, IEEE Microwave Magazine, 14, 5, July 2013, pp. 47-55, 10.1109/MMM.2013.2259394.

6. S. Tedjini, O. Boularess, T. Andriamiharivolamena, H. Rmili, T. Aguili, “A Novel Design of Chipless RFID Tags Based on Alphabets” IEEE MTT-S International Microwave Symposium, June 2017, pp. 1561-1563, doi:10.1109/MWSYM.2017.8058929.

7. S. Genovesi, F. Costa, M. Borgese, A. F. Dicandia, G. Manara, S. Tedjini, E. Perret, “Enhanced Chipless RFID Tags for Sensors Design” IEEE International Symposium on Antennas and Propagation (APURSI), June/July 2016, pp. 1275-1276, doi:10.1109/APS.2016.7696345.

8. S. Tedjini, N. Karmakar, E. Perret, A. Vena, R. Koswatta, R. E-Azim, “Hold the Chips: Chipless Technology, an Alternative Technique for RFID”, IEEE Microwave Magazine, 14, 5, July 2013, pp. 56-65, doi:10.1109/MMM.2013.2259393.

9. A. Vena, E. Perret, S. Tedjini, “RFID Chipless Tag Based on Multiple Phase Shifters” IEEE International Microwave Symposium Digest (MTT), June 2011, doi:10.1109/MWSYM.2011.5972712.